

The Pattern of Supergranular in a Solar Active Region and the Formation of Filaments

V. M. Grigoryev, L. V. Ermakova, and A. I. Khlystova

Institute for Solar–Terrestrial Physics, P.O. Box 4026, Irkutsk, 664033 Russia

Received April 3, 2003; in final form, August 8, 2003

Abstract—The formation of filaments in solar bipolar active regions is investigated, giving particular attention to the relationship between this process and the pattern of supergranular convection. SOHO MDI and Kitt Peak magnetograms and H α filtergrams are used. The large decaying active region NOAA 8525 is considered over the period May 4–7, 1999. The boundaries of supergranules are identified as concentrations of the line-of-sight photospheric field in magnetograms. Filaments in the central part of the active region are studied; as a whole, they are aligned with the supergranule boundaries. Variations in the magnetic field in this period were manifest primarily in the form of “cancellations” and spatial-redistribution processes consistent with the pattern of developing supergranules. These factors created the conditions necessary for the formation of a filament stretched across the entire active region; i.e., the straightening of the polarity-inversion line and reduction of the horizontal gradients of the magnetic field. One possible explanation of the results is that the magnetic-field component along the filament axis is associated with the vortical structure of horizontal flows in the supergranulation cells. © 2004 MAIK “Nauka/Interperiodica”.

1. INTRODUCTION

Quiescent solar filaments lie over polarity-inversion lines (PILs) of the large-scale magnetic field. Studies of the structure of filaments and the surrounding regions in H α (see [1–3] and many other papers) suggest that the magnetic skeleton of a quiescent filament forms a system of arches hooked together, with their ends protruding from the body of the filament and going down into the photosphere (the so-called “feet”). These are clearly visible in large filaments. The feet issue from most filaments to the right in the northern hemisphere and to the left in the southern hemisphere, irrespective of the side from which the filament is viewed. The first type of filaments are called dextral and second type sinistral [2]. These two types of filaments are associated with two directions of the twisting of the filament’s magnetic field—right-handed and left-handed. The structure of filaments suggests that their magnetic fields should have an appreciable axial component. The structure of the chromosphere indicates that the magnetic field in the immediate vicinity of a filament is directed along the filament [1]. Direct measurements of the photospheric magnetic field with moderate spatial resolution indicate that the transverse component of the magnetic field near a filament is mainly directed along the filament, irrespective of whether the filament is quiescent [4, 5] or located in an active region [6]. The formation and stability of such systems can be provided by shear motions.

There is a relationship between the position of the filament and the pattern of the supergranular convection. Based on his analysis of the distances between the feet of filaments, Sykora [7] suggested that the feet are anchored between supergranules, and Plocienia and Rompolt [8] confirmed this result. These studies gave no information about whether the filaments were completely aligned with the boundaries of supergranules or whether they crossed the supergranular cells while being supported in the areas between them. Grigoryev and Ermakova [4, 5] reconstructed the supergranular pattern near a quiescent filament from the line-of-sight velocity field measured with the vector magnetograph of the Sayan observatory, and concluded that the filaments are mainly located over supergranular boundaries.

Investigations of the physical conditions in the solar atmosphere necessary for the formation of quiescent filaments can be considerably aided by studies of filaments in active regions, since they develop in a medium with a strong, rapidly varying magnetic field, making the factors affecting the formation and stability of filaments more clearly manifest. If an active region is large, it will be associated with a pair of cells with positive and negative polarities in maps of the large-scale magnetic field. The filament formed in an active region during the “spotted” stage of its development can be observed over several solar rotations at the PIL of the large-scale magnetic field after the disappearance of the spots.

Maksimov and Ermakova [9, 10] showed that a filament can originate and remain stable in an active region if the PIL is sufficiently long and has a simple shape, and if the magnitudes of the horizontal magnetic-field gradients transverse to the boundary lie within a certain range (Wang and Li [6] came to a similar conclusion). These conditions are satisfied for the PIL separating the leading and following parts of an active region only in the decay stage of the active region. Isolated filamentary fragments can first appear at segments of the PIL where the above conditions are already satisfied, with a full filament forming as the bipolar active region ages. As the active region decays, the mean magnetic-flux density decreases and the PIL straightens. The evolution of the distribution of the line-of-sight magnetic field that is not associated with spots in a bipolar active region can be described analytically over a fairly long period, using some evolutionary parameter that depends on the horizontal gradient of the line-of-sight field averaged over the active region [11]. Therefore, there is a threshold value for the development phase of a bipolar active region, starting from which the horizontal gradients of the line-of-sight magnetic field near the PIL lie within the range favorable for the formation of a filament.

Grigoryev and Ermakova [12] found that a filament in an active region appears after the total spot area has been reduced by about 40%. As the active region evolves, not only the ratio of the magnetic fields of different polarities but also the spatial distribution of the magnetic-field concentration changes. Annular structures delineating the supergranular convection cells are visible in magnetograms of the line-of-sight field in old active regions. Based on their analysis of the line-of-sight velocity field, Grigoryev and Selivanov [13] demonstrated that the supergranular convection is preserved during the formation of a bipolar active region. As a rule, the PIL has a complex shape at this stage, and should intersect supergranules. It is possible that the PIL becomes aligned with the boundaries of convection cells during the decay of the active region and the simplification of the magnetic-field configuration, and that this is one of the necessary conditions for the formation of filaments.

Here, we continue our studies of the development of filaments in bipolar active regions, paying particular attention to elucidating the relationship between this process and the pattern of supergranular convection.

2. OBSERVATIONAL MATERIAL AND THE OBJECT OF OUR STUDIES

The observational material used consists of SOHO MDI and Kitt Peak magnetograms in FITS format

and $H\alpha$ filtergrams from various observatories in GIF format. We considered the active region NOAA 8525, which appeared from beyond the limb on April 29, 1999. According to *Solar Geophysical Data*, the group reached its maximum area (more than 300 mph) on May 2 or 3; its extent was about 20° and its magnetic configuration bipolar. The group consisted of a large leading spot of positive polarity and small spots of both polarities. Subsequently, the area of the group decreases, with the size of the leading spot varying only slightly. During the next rotation, a small spot of positive polarity was situated in the location of the active region, and had decayed by June 6.

This active region had a heliographic position convenient for investigations of the supergranular structure and magnetic field on May 4–6, when its center was in the longitudinal interval E15–W13 at a latitude of N20. We used full-disk Kitt Peak magnetograms for May 4–7 taken once a day and SOHO MDI magnetograms for May 4, 5, and 7 taken at 96-min intervals (the data for May 6 on the website are erroneous). The Kitt Peak magnetograms have a spatial resolution of $1''$ and a sensitivity of 5 G; 55 minutes were required to obtain each magnetogram. The spatial resolution of the MDI magnetograms was about $2''$, and their sensitivity 30 G. Daily Big Bear Solar Observatory $H\alpha$ images available on the website and the Kitt Peak magnetograms were obtained at similar times. We estimate that the quality of the best filtergrams enables location of the ends of filaments to within 3 – $6''$. We considered only filaments lying on the PIL separating the leading and following portions of the active region. The high sensitivity of the Kitt Peak spectromagnetographs ensured high accuracy for the location of the PIL. The boundaries of supergranules were identified in the MDI magnetograms as concentrations of the line-of-sight field in the photosphere. We used the IDL software package to rotate the magnetic images of the Sun to the position of the central meridian in order to directly superpose the images and eliminate the effect of foreshortening. Further, we cut out a $400'' \times 320''$ area that included the entire active region and its neighborhood. The resulting magnetograms were viewed in a slide-show regime. The supergranules are not always clearly defined in the magnetograms; however, the entire time sequence of magnetograms makes it possible to delineate the supergranules fairly confidently, since their lifetimes are substantially longer than the interval between successive MDI magnetograms, and the magnetic fields move along the supergranular boundaries in the course of the evolution.

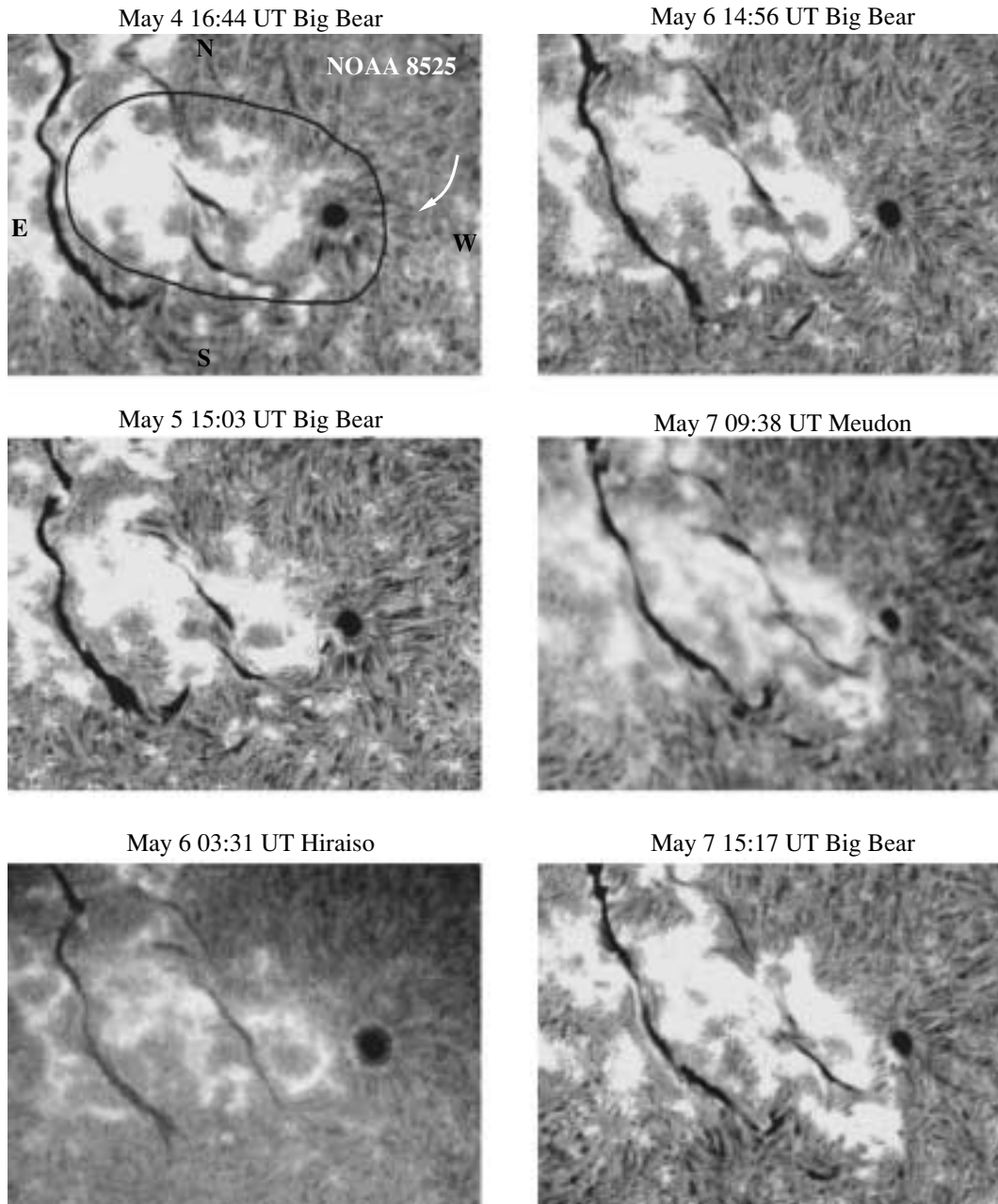


Fig. 1. $H\alpha$ filtergrams.

3. RESULTS AND DISCUSSION

Figure 1 shows fragments of $H\alpha$ filtergrams that include the active region NOAA 8525, while Fig. 2 presents Kitt Peak magnetograms of the line-of-sight field. The filtergrams were obtained with various instruments, making the series appear nonuniform. We consider only filaments located within the active region. These could be observed without difficulty from May 3 to 9; later, they were close to the limb and difficult to identify. The total extent of the filaments was no less than half that of the PIL, and the lengths of the filaments varied. The PIL separating the leading

and following parts of the active region was wavy until May 6, and two filaments that formed near two parallel segments of the PIL deviated substantially from the meridional direction. Later, the PIL was straight and formed a small angle with the meridian. On May 6 at 03:31 UT, a single filament stretched over the entire active region, but subsequently fragmented. Thus, a filamentary channel crossing the entire active region had formed by May 6. By that time, the total spot area in the group was reduced by at least 45%, in agreement with the previously obtained result of [12].

The supergranule contours are superposed on

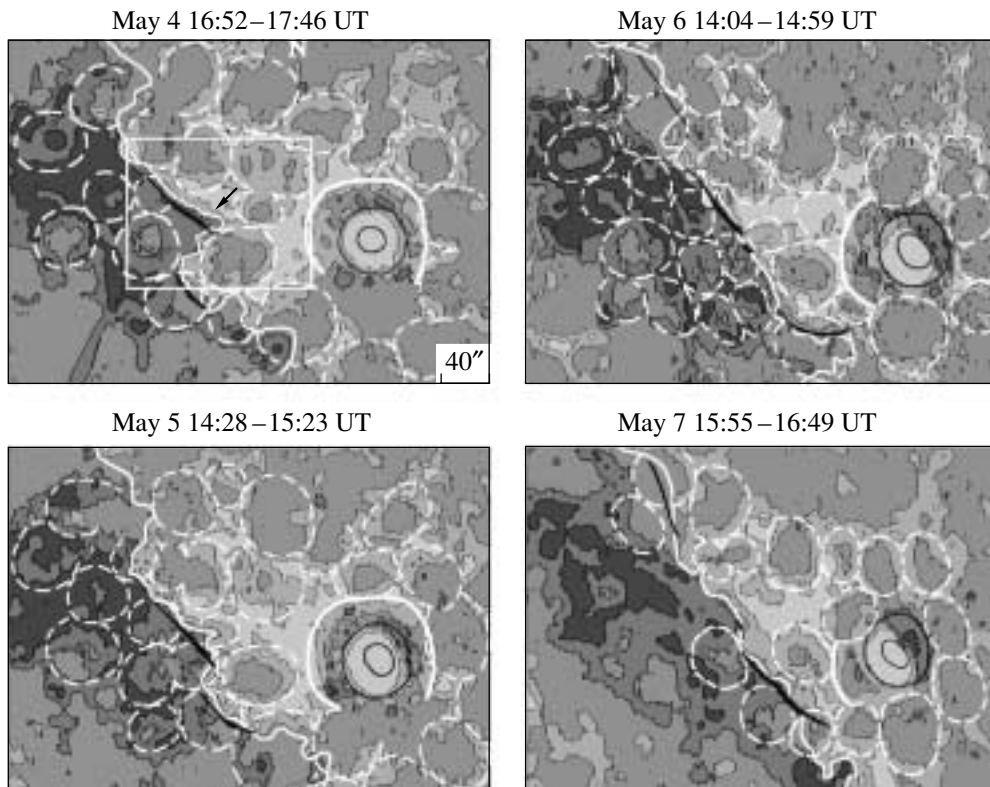


Fig. 2. Kitt Peak maps of the line-of-sight magnetic field with contours of 20 and 180 G. Filaments located using the Big Bear filtergrams and the contours of the umbra and penumbra of the leading spot are shown in black. The polarity-inversion lines (light solid), supergranule contours (dashed), and contours corresponding to the annular convection cell (“moat”) around the leading spot (heavy solid) are shown in white. For other notation, see text.

maps of the line-of-sight magnetic field in Fig. 2. We can see that the filaments in the active region lie near supergranular boundaries and end at places where they join. The lengths of the filaments are initially one to two supergranular diameters and reach three diameters at later times. The available series of MDI magnetograms enables us to analyze the behavior of the supergranular pattern on May 4–5, when the PIL was straightening at the center of the active region.

Figure 3 shows fragments of the magnetograms of the central part of the active region. We can see that three supergranules formed during this period—two with the field of the following polarity and one with the field of the leading polarity. These are labeled 1–3 in order of their appearance. New supergranules formed at the places where the old ones joined in the immediate vicinity of the filament, which remained at its position near the supergranular boundary. Supergranule 2 originated in a high-density magnetic field of the leading polarity, and the pattern of field variations was more pronounced in this case. The first signatures appeared on May 4 at 22:24 UT, as a concavity of both of the magnetic-field contours, and a significant portion of the contour became well defined within three hours. Subsequent changes were manifest as

an extension of the area free of magnetic field within the supergranule and the propagation of the leading-polarity magnetic field along the contour of the supergranule toward the PIL. The diameter increased simultaneously. The leading-polarity field outlined the entire supergranular contour within a day. In their studies of the relationship between the photospheric velocity field and the magnetic-field distribution over the solar surface, Simon *et al.* [14] noted that small magnetic elements on the quiet Sun move toward supergranular boundaries, then drift slowly along these boundaries. Supergranules 1 and 3 originated in the area of the following polarity. According to Fig. 3, the following-polarity magnetic field also drifts along the southern boundary of supergranule 3 toward the PIL. We suppose that the same was true for supergranule 1 at magnetic-field levels below 30 G. Thus, the formation of supergranules near the PIL results in the “convergence” of magnetic fields of opposite polarities, which, according to [15], is a necessary condition for the formation of a filament.

At the same time, the straightening of the PIL is associated with a weakening of the line-of-sight magnetic field and a decrease in the horizontal gradients of the field (Figs. 2, 3). This is due to numer-

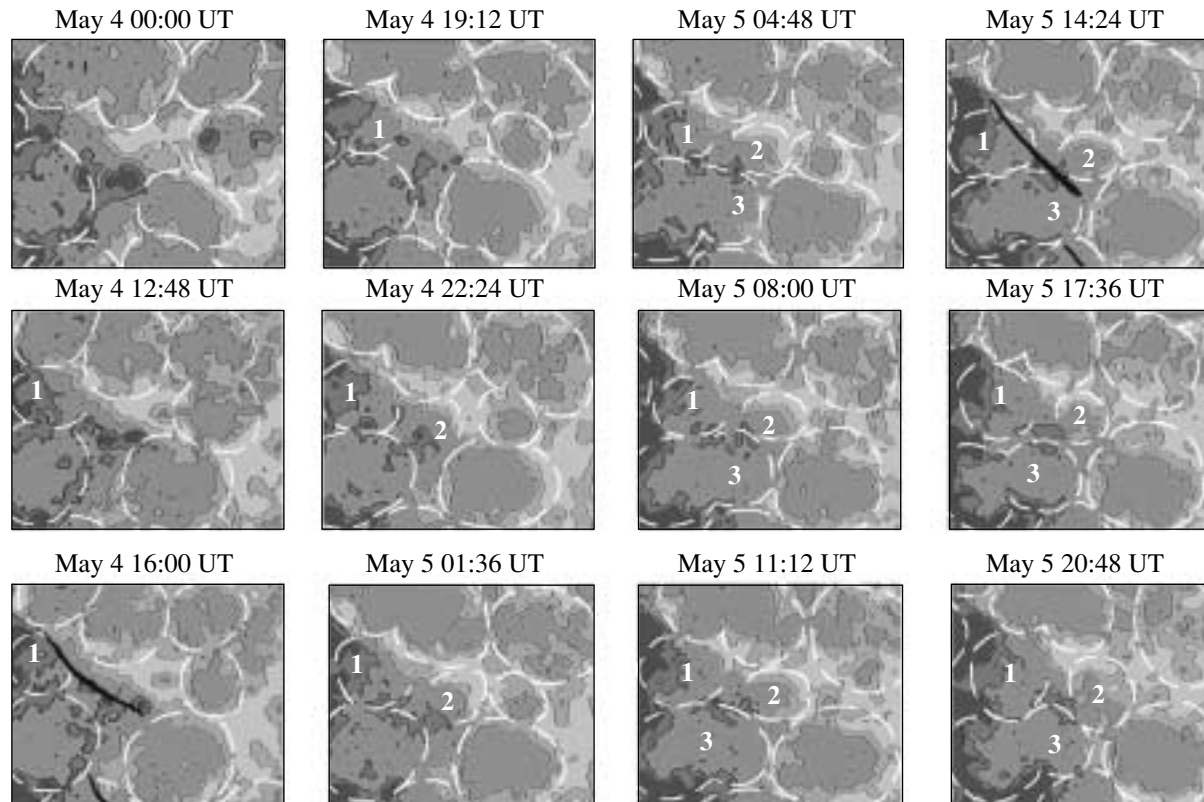


Fig. 3. MDI magnetograms of the central part of the active region marked in Fig. 2. Contours of 30 and 150 G are shown. The notation is the same as in Fig. 2.

ous magnetic-field “cancellation” events. The figures show the presence of field cancellation on May 4 and 5 along the entire PIL, with the cancellation being especially violent near the northern filament, where the magnetic-flux density was higher. One such case is illustrated in Fig. 4; this took place on May 4 to the north of the western part of the northern filament (this region in the active region is shown by an arrow in Fig. 2). The negative pole that underwent cancellation was local, while the opposite pole could not be identified with certainty, except near 16:00 UT; this is typical of cancellation events in the center of an active region [16]. Otherwise, the pattern was quite regular and included a convergence of the poles, increases in the magnetic-field gradient at the site where they came into contact, and the gradual disappearance of the negative pole. The center of supergranule 2 was observed at this location on the following day. North of this filament, cancellation events were observed during the intervals 01:36–12:48 and 17:36–22:24 UT. On May 5, this region corresponded to the center of the new supergranule 3. After the formation of new supergranules, cancellation events occurred when opposite poles moving along the supergranular boundaries toward the PIL collided. Both the very existence of filaments and their instability are associated

with cancellation [16, 17]. They may also play a role in generating the helical structure of the magnetic fields of filaments.

The changes in the convection pattern near the leading spot associated with the evolution of the active region are of interest (Fig. 2). During the initial period, on May 4 and 5, a “moat” with an angular extent of about 270° can be seen around the leading spot in the line-of-sight magnetograms. This is a region of reduced line-of-sight field crossed by small magnetic elements of both polarities moving from the spot toward the surrounding fields [18, 19]. This feature is an annular convection cell that forms around a well-developed spot and transfers excess heat outward from the base of the spot, thereby stabilizing it [20, 21]. The moat around the leading spot broke down gradually over the next two days; on May 7, the arc of the moat was about 60° . The supergranular convection in the immediate vicinity of the spot was simultaneously reestablished (Fig. 2). No substantial changes in the shape and area of the leading spot occurred during that period. Moats are primarily associated with decaying spots; however, many reports of moats around growing spots can also be found in the literature. The formation of a moat at the end of the growth stage of main spots whose area exceeded

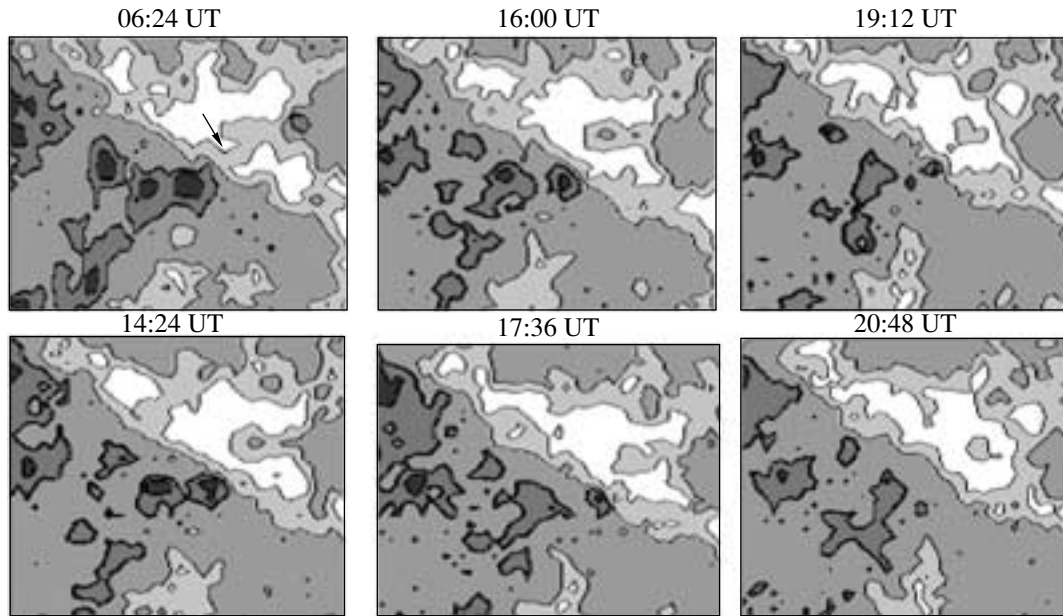


Fig. 4. MDI magnetograms (contours of 30 and 150 G are shown) for May 4 illustrating the cancellation of magnetic flux.

that of a supergranule is described in [13, 22]. It is likely that the development of a large spot ends with the formation of such a cell. In the case considered here, the moat was first observed on May 3, near the maximum development of the active region. This suggests that the formation and decay of a moat not only determine a spot state, but also characterize the intensity and state of the entire flux tube forming the active region; i.e., they represent a characteristic phase in the growth of the active region.

Thus, in the decay stage of a bipolar active region, magnetic flux is lost due to cancellation in the central part of the region at the line where the magnetic fields of opposite polarities come into contact; simultaneously, motions in the newly forming supergranules result in a spatial redistribution of the flux. These factors straighten the PIL and reduce the horizontal gradients of the magnetic field. An extended filamentary channel forms near the PIL. The developing filaments are aligned with supergranular boundaries.

A number of observational conditions required for the formation and existence of a filament are known. We emphasize here three of these that are directly related to the structure of the magnetic field in the filament.

(1) Filaments are located along the line separating different magnetic polarities.

(2) A magnetic-field component associated with filaments and aligned with the PIL is present; this is indicated by the structure of the fibrils in chromospheric rosettes near filaments and filamentary channels [2], as well as by direct measurements of the photospheric magnetic fields [4–6].

(3) The supergranular cells near a filament form an almost regular pattern, with supergranules arranged along the PIL [4, 5] (this can also be seen from our results).

To explain these observational facts, we suggest that the formation of the component of the magnetic

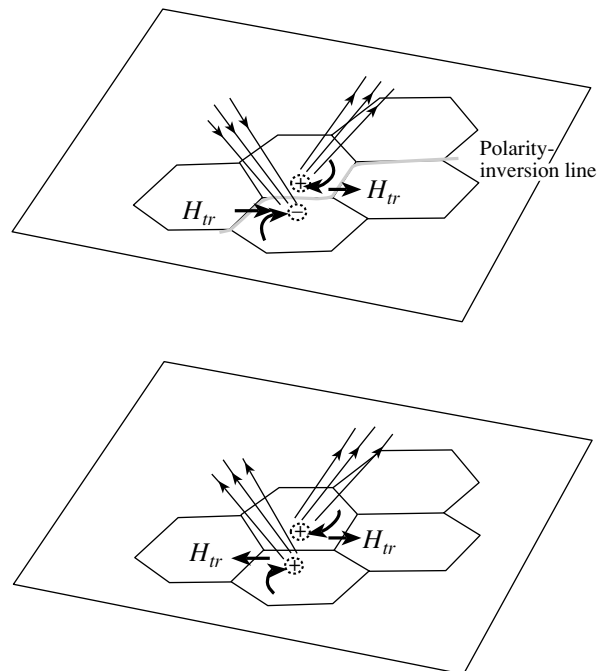


Fig. 5. Schematic of the formation of the axial component of the magnetic field under the action of the vortical component of the motions in supergranules.

field aligned with the PIL is related to the vortical structure of the horizontal flows in supergranular cells (Fig. 5). The vortical structure in a supergranule results from the action of the Coriolis force on the horizontal divergence of the flow. If supergranules are arranged along a PIL, the vortical flows from neighboring supergranules converging to this line squeeze together the magnetic fields of opposite polarities, leading to the disappearance of the vertical component of the field; the observed magnetic-flux cancellation events provide evidence for this effect. This reduces the magnetic-field gradient at the PIL (so that the necessary condition for the formation of filaments is satisfied [9]). At the same time, the magnetic field component aligned with the PIL is increased, since the vortical component of the flows in the neighboring supergranules has opposite directions on either side of the PIL. This ensures the presence of a filament-aligned component of the field. This hypothesis is supported not only by our results concerning the structure of supergranular cells, but also by a theoretical consideration of cellular convection in a rotating fluid [23]. The first evidence for the rotation of cells was presented by Kubičela [24]. Using modern techniques, Duvall and Gizon [25] recently confirmed the effect of the Coriolis force on supergranular flows. They estimated the quantity curl/div and found that it varies with latitude from 0 at the equator to ± 0.07 at latitudes of $\pm 60^\circ$. In addition, studies of motions in supergranules based on the advection of mesogranules [26] yield horizontal velocities of 500–1000 m/s, which provides an energetically more convincing argument for the possibility that the flows affect the magnetic field, compared to the velocities of 350–500 m/s determined earlier.

Our hypothesis requires further development. However, it can also provide a natural explanation for certain additional features, such as the disappearance of magnetic knots at the polarity-inversion line, the lack of filaments in the equatorial zone, and the presence of intense filaments at high latitudes.

ACKNOWLEDGMENTS

This work was supported by the program “Leading Scientific Schools of Russia” (grant NSh-733.2003.2) and the Federal Science and Technology program “Astronomy.”

REFERENCES

1. P. Foukal, *Solar Phys.* **19**, 59 (1971).
2. S. F. Martin, R. Bilimora, and P. W. Tracadas, *Solar Surface Magnetism*, Ed. by R. J. Rutten and C. J. Schrijver (Kluwer, 1994), p. 303.
3. S. F. Martin, *Solar Phys.* **182**, 107 (1998).
4. V. M. Grigoryev and L. V. Ermakova, *Current Problems in Solar Cyclicity*, Ed. by V. I. Makarov, V. N. Obridko, *et al.* (GAO RAN, St. Petersburg, 1997), p. 317 [in Russian].
5. V. M. Grigoryev and L. V. Ermakova, *Astron. Astrophys. Trans.* **17**, 355 (1999).
6. Wang and W. Li, *New Perspectives of Solar Prominences*, Ed. by D. Webb, D. Rust, and B. Schmieder; ASP Conf. Ser. **150**, 98 (1998).
7. J. Sykora, *Bull. Astron. Inst. Czechosl.* **19**, 37 (1968).
8. S. Plocienia and B. Rompolt, *Solar Phys.* **29**, 399 (1973).
9. V. P. Maksimov and L. V. Ermakova, *Astron. Zh.* **62**, 558 (1985) [*Sov. Astron.* **29**, 323 (1985)].
10. V. P. Maksimov and L. V. Ermakova, *Astron. Zh.* **64**, 841 (1987) [*Sov. Astron.* **31**, 438 (1987)].
11. L. V. Ermakova, *Solar Phys.* **191**, 161 (2000).
12. V. M. Grigoryev and L. V. Ermakova, *New Solar Activity Cycle: Observational and Theoretical Aspects*, Ed. by V. I. Makarov, V. N. Obridko, *et al.* (GAO RAN, St. Petersburg, 1998), p. 233 [in Russian].
13. V. M. Grigoryev and V. L. Selivanov, *Contrib. Astron. Observ. Skalnaté Pleso* **15**, 87 (1986).
14. G. W. Simon, A. M. Title, K. P. Topka, *et al.*, *Astrophys. J.* **327**, 964 (1988).
15. S. Martin, *Dynamics of Quiescent Prominences*, Ed. by Ruzdjak and E. Tandberg-Hanssen (Springer-Verlag, 1990); *Lect. Notes Phys.* **363**, 1 (1990).
16. S. F. Martin, S. H. B. Livi, and J. Wang, *Austral. J. Phys.* **38**, 929 (1985).
17. J. Wang, Z. Shi, and S. F. Martin, *Astron. Astrophys.* **316**, 201 (1996).
18. D. Vrabc, *IAU Symp. No. 56: Chromospheric Fine Structure*, Ed. by R. G. Athey (Reidel, Dordrecht, 1974), p. 201.
19. K. Harvey and J. Harvey, *Solar Phys.* **28**, 61 (1973).
20. F. Meyer, H. U. Schmidt, N. D. Weise, *et al.*, *Mon. Not. R. Astron. Soc.* **169**, 35 (1974).
21. A. Nye, D. Brunning, and B. J. Labonte, *Solar Phys.* **115**, 25 (1988).
22. L. V. Ermakova, *The Magnetic and Velocity Fields of Solar Active Regions*, Ed. by H. Zirin, G. Ai, and H. Wang; ASP Conf. Ser. **46**, 75 (1993).
23. G. Veronis, *J. Fluid Mech.* **5**, 401 (1959).
24. A. Kubicela, *Solar Activity and Related Interplanetary and Terrestrial Phenomena* (Proc. 1st European Astron. Meeting), Ed. by J. Xanthakis (Springer, Berlin, 1973), p. 123.
25. T. L. Duvall, Jr. and L. Gizon, *Solar Phys.* **192**, 177 (2000).
26. R. A. Shine, G. W. Simon, and N. E. Hurlburt, *Solar Phys.* **193**, 313 (2000).

Translated by A. Getling